Light Metals 2014
Edited by: John Grandfield
TMS (The Minerals, Metals & Materials Society), 2014

ANODE ELECTRICAL RESISTANCE MEASUREMENTS: LEARNING AND INDUSTRIAL ON-LINE MEASUREMENT EQUIPMENT DEVELOPMENT

Guillaume Léonard[1], Sébastien Guérard[1], Denis Laroche[1], Jean-Claude Arnaud[2], Stéphane Gourmaud[3], Marc Gagnon[4], Marie-Josée Chollier[1] and Yvon Perron[1]
[1]Rio Tinto Alcan - Arvida Research and Development Centre, 1955 blvd Mellon, Jonquière, Québec, G7S 4K8, Canada
[2]Rio Tinto Alcan - Aluval, 725, rue Aristide Bergès, BP 7, 38341 Voreppe Cedex, France
[3]ECL™, 100 rue Chalant, 59790 Ronchin, France
[4]Aluminerie Alouette Inc., 400 chemin de la Pointe-Noire, P.O. Box 1650, G4R 5M9, Canada

Keywords: Carbon resistivity, Anode resistance, Anode voltage drop, On-line measurement

Abstract

The electrical resistance of anodes is recognized as a significant parameter for pot performance as the carbon material itself contributes to half of the anode assembly voltage drop. An R&D apparatus for measuring the anode electrical resistance (MIREA) was recently developed by Rio Tinto Alcan. In the last two years, six measurement campaigns were held at different anode plants around the world during which more than 600 anodes were characterized. The MIREA apparatus used during these campaigns helped to highlight resistance heterogeneity problems such as highly resistive tops and helped to detect non-optimized vibroformers. A better understanding of the resistance variability was acquired during these campaigns and justified the development of the apparatus at an industrial scale. The 2nd Generation MIREA was developed to allow smelter process teams to monitor electrical resistance of all anodes produced. This equipment was designed to reliably achieve more than one anode measurement per minute and to deliver comprehensive data interpretation.

Introduction

Anode electrical resistance is increasingly recognized as a key parameter for pot operation, as the carbon material itself contributes close to 50% of the anode assembly voltage drop[1]. The current method to measure anode resistance is described in the ISO standard 11713[2]. The method is based on the resistivity measurement of an anode core sample. However, coring operations are time-consuming, destructive and provide limited information on the spatial variability within an anode. For example, cracks in a specific anode section could remain undetected due to the absence of sampling in that specific region.

The position of an anode defect has an influence on the overall anodic electrical consumption. A defect in the anode upper section will penalize the anode voltage drop throughout the entire electrolysis cycle. In contrast, an anomaly in the lower anode section will be consumed in the early days of the electrolysis cycle and thus will have a reduced influence on the mean anode voltage drop.

For the reasons mentioned above, an instantaneous and non-destructive R&D device (MIREA; Figure 1) was recently developed by Rio Tinto Alcan to study the contribution of different anode sections on the anodic electrical resistance. The MIREA acronym is derived from a French translation of "Instantaneous Measurement of Anodic Electrical Resistance". The device was presented by Chollier-Brym et al. in a previous paper[1]. Comparisons were made between MIREA measures and an intensive anode coring campaign. The paper also investigated the influence of two forming processes (press and vibroformer) on the anode electrical resistance.

The particularity of the MIREA technology over other resistivity measurement methods such as electrical resistance tomography[3,4] or electrical resistivity surveys[5], is that it replicates the current distribution of an anode in service. The MIREA device puts an emphasis on the critical role of the stub holes area to the anode electrical resistance. Thus, it allows a characterization of the anode electrical properties under the same current flow patterns as those found during electrolysis.

This work is a continuation of the previous study of Chollier-Brym et al.[1]. It presents the insights of six MIREA campaigns which took place, worldwide, at different anode plants, in 2012-2013. In total, more than 600 anodes of nine different formats were characterized. Key findings range from the detection of non-optimized vibroformers to the presence of resistance heterogeneity within an anode format. These campaigns also offered a basis of comparison between plants to assess their performance in terms of anode electrical resistance. Globally, these findings provided a better understanding of the resistance variability found in an individual anode as well as in a whole anode population. Finally, this paper presents the development of the 2nd Generation MIREA device (On-Line Industrial MIREA), which will be commissioned to Aluminerie Alouette, in 2014. This on-line device will offer the possibility to take proactive actions to improve the quality of the anode population produced by the smelter.

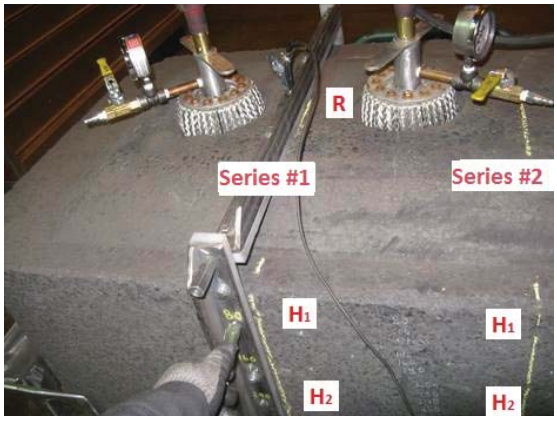

Figure 1. MIREA setup with the pneumatic devices and the measurement position template.

Measurement methodology

The MIREA setup, shown in Figure 1, replicates the anodic current distribution during electrolysis using pneumatic devices (metallic balloons) imitating the standard anodic rodding. These balloons, pressurized in the stub holes, establish a mechanical connection with the anode, thereby allowing the passage of an electric current produced by a portable power source. The electric circuit is closed with a metallic brush carpet in contact with the anode bottom surface. A voltmeter is then used to establish a voltage drop map of the anode side surface. Voltage drops are measured between reference point (R) located on the anode top and at predefined positions on the anode surface.

For all campaigns presented in this paper, the voltage drop measures were taken following a template consisting of two series (Series 1 and Series 2) of measures. These series were located between the stub holes and corresponded to the left and right anode sides, as illustrated in Figure 2.

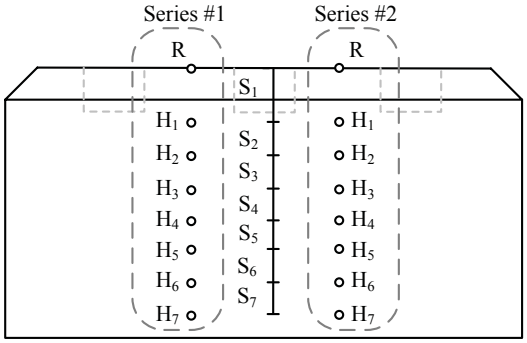

Figure 2. MIREA measurement position template (generic anode format).

For each series, the voltage drop ($\Delta V_{R\text{-}Hi}$) was measured between the reference point (R) and a predefined height position (H_1 to $H_{6\text{ or }7}$). This sampling methodology provided 12-14 measures per anode and was considered a good trade-off between the measuring cadence and the anode representativeness. Voltage drop data were averaged between the two series for each H_i position. Table 1 presents the parameters collected during a MIREA measurement.

Table 1.MIREA measurement parameters.

Anode height position, H_i	Voltage drop, $\Delta V_{R\text{-}Hi}$	Slice, S_i	Slice voltage drop, $\Delta V(S_i)$
R - H_0	-		
		S_1	$\Delta V_{R\text{-}H1}$
H_1	$\Delta V_{R\text{-}H1}$		
		S_2	$\Delta V_{R\text{-}H2}$-$\Delta V_{R\text{-}H1}$
H_2	$\Delta V_{R\text{-}H2}$		
		S_3	$\Delta V_{R\text{-}H3}$-$\Delta V_{R\text{-}H2}$
H_3	$\Delta V_{R\text{-}H3}$		
		S_4	$\Delta V_{R\text{-}H4}$-$\Delta V_{R\text{-}H3}$
H_4	$\Delta V_{R\text{-}H4}$		
		S_5	$\Delta V_{R\text{-}H5}$-$\Delta V_{R\text{-}H4}$
H_5	$\Delta V_{R\text{-}H5}$		
		S_6	$\Delta V_{R\text{-}H6}$-$\Delta V_{R\text{-}H5}$
H_6	$\Delta V_{R\text{-}H6}$		
		S_7	$\Delta V_{R\text{-}H7}$-$\Delta V_{R\text{-}H6}$
H_7	$\Delta V_{R\text{-}H7}$		

Millivolt measures on the anode surface are converted to apparent resistivity values to provide a physical grasp of the MIREA data and allow comparisons between different anode formats. Numerical simulations modeling the electrical potential drop on the anode surface are used for this conversion. The simulations are based on the anode blueprint and use a constant resistivity value of 60 μΩm. One simulation of a generic anode format is illustrated in Figure 3.

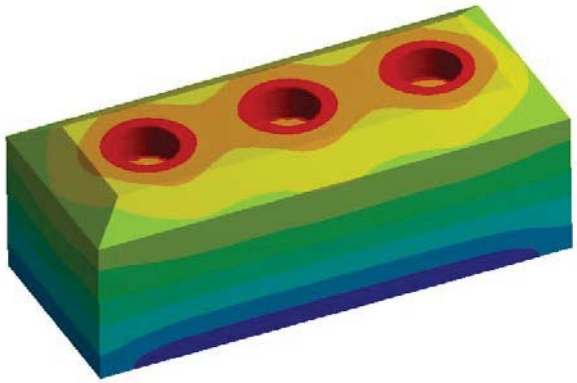

Figure 3. Numerical simulation of a generic anode format showing the voltage drop on the anode surface.

To make the resistivity conversion, it is assumed that the resistivity of an anode slice section, S_i, is proportional to the slice voltage drop, $\Delta V(S_i)$, measured between the slice boundaries H_{i-1} and H_i (Table 1 and Figure 2). The proportionality factor of this relation is the ratio between the simulation resistivity (ρ_{sim}) and the simulated voltage drop of S_i, $\Delta V_{sim}(S_i)$:

$$\rho(S_i) = \frac{\rho_{sim}}{\Delta V_{sim}(S_i)} \Delta V(S_i)$$

It must be noted that this assumption is valid if the current distribution in the real-life anode is similar to that of the simulated case. However, some biases are always present between the real and simulated current distribution due to the heterogeneity of the real-life anode. Therefore, this document continually refers to an apparent resistivity value when presenting resistivity data.

Results and discussions

This section is divided into five parts describing key findings of the MIREA worldwide campaigns:

- detection of individual anodes with defects,
- comparison between the right and left anode sides,
- comparison of an anode format produced at two different plants (non-optimized vibroformers),
- comparison between different anode formats,
- comparison between visual rejection criteria and MIREA data.

These findings range from the detection of anode with defaults to the comparison between smelters to assess their performance in terms of anode electrical resistance.

Detection of individual anodes with defects

Figure 4 shows the "mV" fingerprints collected by the MIREA device for anodes produced by the same plant. Each data point represents the cumulated voltage drop (ΔV_{R-Hi}) between the reference point (R) and an anode height position (H_i). Values are averaged between Series 1 and 2. This figure allows the detection of anodes with important resistance defects. As can be seen, four "outlier" anodes deviate from the "normal" anode population. These deviations indicate the presence of important defects. These anodes should be discarded and recycled by the anode plant since they can compromise the normal pot room operations.

For the "normal" population, it can be observed that the voltage drop distribution in the upper anode section (H_1 to H_3) is narrower than for the lower anode sections (H_4 to H_7). This phenomenon is explained by the accumulation of resistance artifacts along the anode height.

The conversion of the "mV" data into a global apparent resistivity value, for an entire anode, can be estimated using the cumulated voltage drop measure between R and H_7. For the "normal" anodes presented in Figure 4, ΔV_{R-H7} varies between 8.0 and 9.7 mV. These values can be translated into a global anode apparent resistivity range of 62 to 68 μΩm.

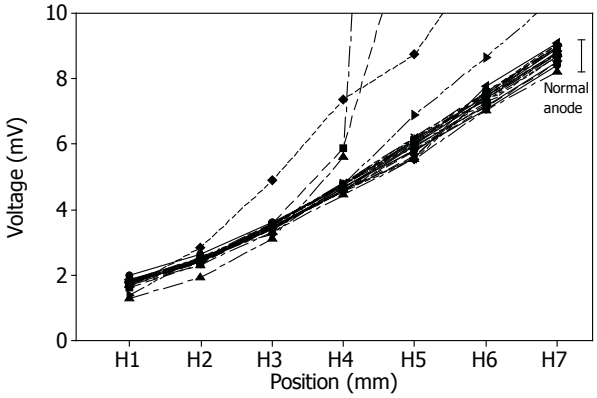

Figure 4. MIREA cumulated "mV" measures as a function of the measurement height positions.

Figure 5 presents a resistivity analysis according to the slice sections of an anode. Millivolt data found in Figure 4, for the "normal" population, are converted into resistivity values. The points found on the curves represent the apparent resistivity of an anode slice section (S_i). This transformation of "mV" data into apparent resistivity value allows an easier detection of smaller anodic defects that were not easily visible in Figure 4. Discontinuities were found for "normal" anodes in lower slice sections. Indeed, three anodes had resistance anomalies in slice section #6 and another one in slice section #5. These anomalies are attributed to the presence of anode defects and cracks in those specific sections. For these three anodes, it must also be mentioned that the resistance defects had not been visually detected.

The resistivity defects found in the three anodes are not significant enough to discard those anodes from the pot rooms, since the estimated voltage drop penalization is insufficient to justify the anode recycle operation. However, with the MIREA insight, it is possible to determine if these discontinuities localized in sections #5 and #6 are systematically present in an important fraction of the overall anode population. With this knowledge, actions can be taken by the anode plant process team to reduce the occurrence of these defects and thus lower the electrolysis voltage drop average of the anode population. This resistivity improvement will be translated into an energy reduction cost for the smelter.

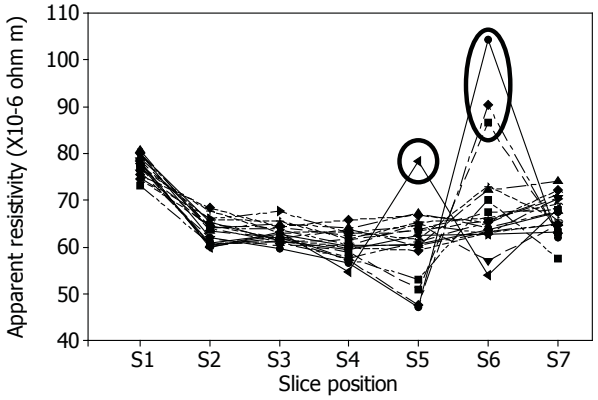

Figure 5. Anode resistivity profile for the "normal" anode population presented in Figure 4.

Comparison of an anode format produced at two different plants (non-optimized vibroformers)

A second example of possible energy cost reductions was found during another campaign where anodes of the same format, produced by two different anode plants, were evaluated using the MIREA device. Figure 6 gives a comparison of the apparent resistivity fingerprint of both plants. Intervals on the graph illustrate the 95% confidence intervals on the apparent resistivity means for six anode slices. Both groups were measured during the same time period with the same MIREA equipment and operators.

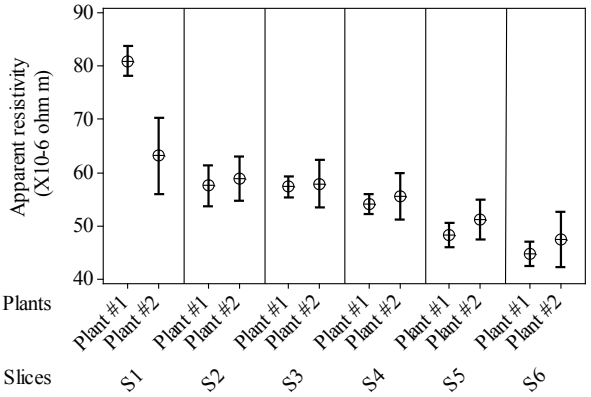

Figure 6. Comparison of two plants producing an identical anode format. Intervals illustrate the 95% confidence intervals on the means for six anode slices.

An important gap in apparent resistivity (≈17 μΩm) is observed in the anode top section (S_1). Below S_1, anodes produced by Plant #1 are not significantly different from those of Plant #2. The fact that anodes from Plant #1 perform well below the anode top does not eliminate the resistance loss found in the anode top section. This anode section will always be present and therefore will penalize the anode voltage drop throughout the entire electrolysis

cycle. Thus, efforts must be made to attenuate this discrepancy. At the moment, some hypotheses are proposed to explain this discrepancy and are linked to difference in operation related to the vibroformer counter pressure and vacuum parameters.

Comparison between the right and left anode sides

Using the data gathered from multiple campaigns, it was found that some anode formats had systematic resistivity differences between the left and right anode sides (Series #1 vs. Series #2). This finding was unexpected since both measurement series are taken in the mid anode section (Figure 2). These differences were even observed for an anode format having a relatively minor shape asymmetry.

Table 2 shows the results of pairwise Student t tests used to find these discrepancies. The table contains results of two anode formats coming from two different plants. For Plant #1 (n=160 anodes), significant differences of 5.0 and 5.6 μΩm were found (see the asterisk "*" mark) in the lower parts of the anode format (S_6 and S_7). This is an indication of the presence of systematic heterogeneities in the anode population. As for Plant #2 (n=59), no statistically significant differences between the right and left sides were observed in the anode population.

Table 2. Pairwise Student t tests between Series #1 and #2.

Slice	Plant #1		Plant #2	
	Δ (μΩm)	P-value	Δ (μΩm)	P-value
S_1	0.5	0.25	< 0.05	0.94
S_2	< 0.05	0.99	0.4	0.52
…	…	…	…	…
S_6	5.0	< 0.001*	< 0.05	0.92
S_7	5.6	< 0.001*	-	-

However, it is important to remember that the resistivity differences found for some anode formats are only qualitative since the assumption of similar current distribution between the real and simulated anode can be challenged in this case.

At this moment, three hypotheses are proposed to explain the presence of systematic differences between the left and right anode sides for some anode formats. The first hypothesis is related to an uneven distribution of the carbon paste in the mould box before the forming process. The second and third hypotheses are based on an uneven vibration of the vibroformer or an unbalanced cover weight during forming.

Comparison between different anode formats

Apparent resistivity profiles of all anode formats measured with the MIREA device are illustrated in Figure 7. Each curve represents the averaged resistivity profile of an anode format and is based on "normal" population. For example, the curve identified with the asterisk "*" mark represents the averaged anode population of the format presented in Figure 5.

It is interesting to note the wide variety of performance in terms of apparent resistivity for the different anode formats. The anode resistivity profiles generally follow a decreasing pattern along the anode height (H_1 to H_6-H_7). The most resistive anode format passes from an apparent resistivity value of 136 μΩm, in the anode top, to 68 μΩm, in the anode bottom part. In contrast, the best anode format reaches apparent resistivity values of the order of 63 and 45 μΩm in the anode top and bottom part, respectively. Therefore, the worst anode format is 50% more resistive in the lower anode section than the best anode format. When considering the anode tops, this difference reaches 115%.

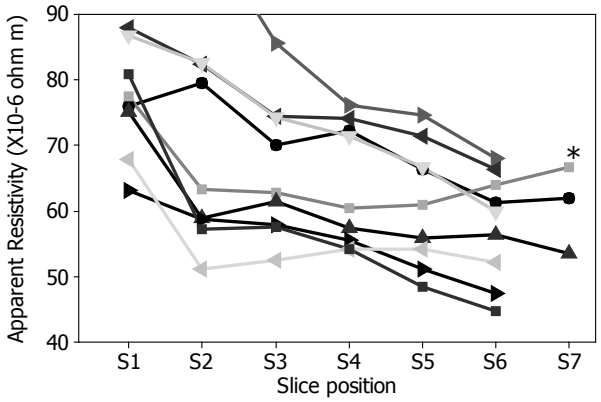

Figure 7. Anode apparent resistivity profiles for different anode formats.

As for the variability of the populations, Figure 8 illustrates the global apparent resistivity distribution of four anode formats. These distributions were built using the parameter $\Delta V_{R\text{-}H7}$ to estimate the apparent resistivity of the entire anode and were based on anodes considered "normal". Three out of the four populations of Figure 8 show a bell shape distribution with some apparent skewness. However, statistical tests on the normality of the population did not detect the presence of non-normal distribution. Additional data will be needed to determine if anode populations do indeed follow normal distributions. A certain degree of skewness is expected, especially for low resistive anode formats, as there is a physical limit to the low resistivities that can be obtained. However, upper resistivity anodes are not constrained and can reach high values.

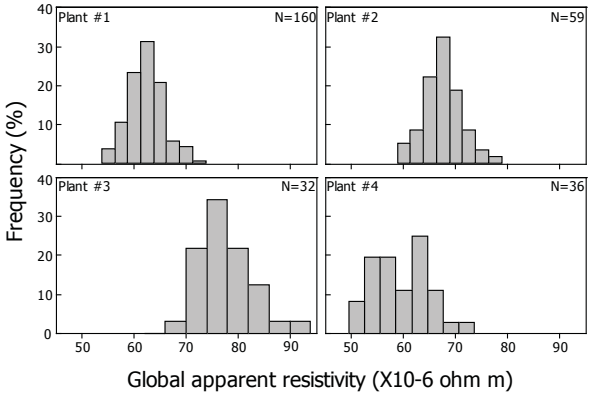

Figure 8. Global apparent resistivity distribution of different anode formats.

Comparison between visual rejection criteria and MIREA data

Finally, in one campaign, a problematic anode lot was deliberately chosen to compare the MIREA measurement technique with that of the visual observation technique. The visual observation made on the anode was related to the presence of stub/vertical/horizontal cracks, segregation, agglomerated packing coke, etc. This information was then used to classify the anode in

a “quality” category: "Good", "Normal", "Fair-Mediocre", and "Rejected". For example, in the "Good" category, no anode had apparent defects with the exception of agglomerated packing coke on the anode surface. For the "Normal" category, half of the anodes had horizontal cracks. As for the “Faire-Mediocre” category, 88% of the anodes had horizontal cracks. It must be mentioned that the number of anodes measured for each “quality” class did not represent the distribution of the problematic anode lot. An effort was made to measure more “Fair-Mediocre” anodes to access their overall performance in terms of resistivity.

A hammer test was also performed on each anode to evaluate its quality. The "sound" produced by the anode after the impact with a hammer was qualified according to a good or bad scale. The "good" level corresponded to a sound with resonance, while the "bad" level corresponded to a rapid attenuation of the sound after impact. It should be noted that when an attenuated sound was recorded, the anode was automatically discarded to the "rejected” category.

Table 3 shows a comparison of these visual “quality” classes with the MIREA results. This comparison is made by using the four quartiles of the “Fair-Mediocre” population results ($\Delta V_{R\text{-}H7}$) to discriminate the other visual “quality” category. For example, 28% of the “Good” anode population had $\Delta V_{R\text{-}H7}$ values within the third quartile of the “Fair-Mediocre” population.

The analysis of Table 3 shows that the "Good" anode population is mainly distributed in the first three quartiles of the “Fair-Mediocre” population and not only in the first quartile. The presence of a large number of “Good” anodes in the second and third quartiles indicates that many of them show a resistivity performance level similar to that of the “Fair-Mediocre” population. Thus, several anodes in the “Normal” and “Fair-Mediocre” categories obtain similar results to those of the best “Good” anodes. Indeed, the "Fair-Mediocre" category contains proportionally as many anodes in the first quartile than the “Good” population. For the “Rejected” population, 85% of the anodes are regrouped in the last quartile with some of the “Fair-Mediocre” anodes and even with some “Good” anodes.

Table 3. Distribution of the anode population according to the visual observation and the MIREA measures $\Delta V_{R\text{-}H7}$.

Quartile (MIREA)	Anode quality classes “Visual observations”			
	“Good”	“Normal”	“Fair-Mediocre”	“Rejected”
1er	23 %	30 %	25 %	0 %
2e	39 %	25 %	25 %	10 %
3e	28 %	36 %	25 %	5 %
4e	10 %	9 %	25 %	85 %
NBR	31	33	96	20

Globally, visual observation and the hammer test effectively discriminate "rejected" anodes from the overall population. However, the performance prediction of "Good", "Normal" and "Fair-Mediocre" anodes, based on visual observation, remains unproven from the point of view of the MIREA results. It should also be remembered that the detection of minor resistivity defects such as the anomalies presented in Figure 5, are not possible when relying on visual observation alone.

These results show the need to consider automating the MIREA device to avoid misclassification of anodes when relying on visual observation only. An on-line MIREA device could also reduce drastically the labor cost associated with visual anode monitoring.

2nd Generation MIREA (On-Line Industrial MIREA)

The results obtained with the R&D MIREA device provided a better understanding of the resistance variability in an anode population and showed the possibility of discarding problematic anodes without relying exclusively on visual observation. Indeed, the performance prediction of anodes, based on visual observation, remains unproven in the point of view of the MIREA results.

These findings justified the development of the apparatus on an industrial scale. Thus, a 2nd Generation MIREA (On-Line Industrial MIREA) was developed to allow smelter process teams to monitor electrical resistance of all the anodes produced. This 2nd Generation MIREA device will be commissioned in 2014 to Aluminerie Alouette for test trials. This industrial pilot is the result of technological development partnership between Rio Tinto Alcan (Technology, Research and Development, ECL™) and Aluminerie Alouette.

The industrial device was designed to reliably achieve more than one anode measurement per minute. It will be completely automated and will require limited maintenance. It will also include an independent power source for each stub hole to improve accuracy. The “mV” measurement position template will include four measure series with seven predefined height positions. In total, 28 “mV” measures will be taken for each anode, for better anode representativeness. The data interpretation will include algorithms to detect anodes with defects and will produce comprehensive reports to monitor the performance and variability of the anodes manufactured in specific time periods. This increment in process understanding will be used to improve the quality of the anode population produced by an anode plant. It will also potentially allow smelters to take proactive actions for the electrolysis process; for example by rejecting highly resistive anodes destroying value or by compensating the cell voltage target.

Conclusion

After more than 600 anodes measured with the R&D MIREA apparatus from nine different anode formats, it can be concluded that a better understanding of the resistivity variability in an individual anode as well as in a whole anode population was achieved. The R&D MIREA device highlighted resistance heterogeneity problems such as highly resistive tops and helped detect non-optimized vibroformers. The MIREA campaigns also offered a basis of comparison between plants to assess their performance in terms of anode electrical resistance.

The 2nd Generation MIREA device, developed for an industrial measurement cadence, will provide a deeper understanding of this variability in coming years. This increment in process understanding will be used to improve the quality of the anode population produced by an anode plant. It will also potentially allow smelters to take proactive actions concerning the electrolysis process.

Acknowledgements

The authors would like to acknowledge the work of A. Alexandre, M. Landry, C. Simard, L. Simard, D. Ringuette, N. Letendre, B. Brassard and D. Lepage during the MIREA campaigns. The authors also wish to acknowledge the numerous contributors of the Rio Tinto Alcan Reduction R&D team for their ingenuity and tenacity which resulted in the development of the MIREA device. Finally, the help of S. de Moor in reviewing the manuscript is greatly appreciated.

References

1. M.J. Chollier-Brym, D. Laroche, A. Alexandre, M. Landry, C. Simard, L. Simard and D. Ringuette, "New method for representative measurement of anode electrical resistance", Light Metals, (2012), 1299-1302.

2. ISO 11713, "Carbonaceous materials used in the production of aluminium - Cathode blocks and baked anodes - Determination of electrical resistivity at ambient temperature", International Organisation for Standardization, (2000).

3. M. Sharifi and B. Young, "Electric resistance tomography (ERT) applications to chemical engineering", Chemical Engineering Research and Design, (2013), Article in press.

4. F. Dickin and M. Wang, "Electrical resistance tomography for process applications", Measurement Science and Technology, 7 (1996), 247-260.

5. M.H. Loke, "Electrical resistivity surveys and data interpretation" in Gupta, H (ed.), Solid Earth Geophysics Encyclopaedia (2nd Edition) "Electrical & Electromagnetic" Springer-Verlag, (2011), 276-283.